PAPER • OPEN ACCESS

A scheme for multipartite entanglement distribution via separable carriers

To cite this article: Alessandro Laneve *et al* 2022 *New J. Phys.* **24** 123003

IOP Publishing New J. Phys. 24 (2022) 123003 https://doi.org/10.1088/1367-2630/aca499

New Journal of Physics
The open access journal at the forefront of physics

Deutsche Physikalische Gesellschaft DPG
IOP Institute of Physics

Published in partnership with: Deutsche Physikalische Gesellschaft and the Institute of Physics

OPEN ACCESS

RECEIVED
8 July 2022

REVISED
27 October 2022

ACCEPTED FOR PUBLICATION
21 November 2022

PUBLISHED
11 January 2023

PAPER

A scheme for multipartite entanglement distribution via separable carriers

Alessandro Laneve[1], **Hannah McAleese**[2] and **Mauro Paternostro**[2,*]

[1] Dipartimento di Fisica, Sapienza Università di Roma, Piazzale Aldo Moro, 5, I-00185 Roma, Italy
[2] Centre for Quantum Materials and Technologies, School of Mathematics and Physics, Queen's University Belfast, BT7 1NN Belfast, United Kingdom
* Author to whom any correspondence should be addressed.

E-mail: m.paternostro@qub.ac.uk

Keywords: quantum networking, quantum correlations, entanglement distribution, thought experimental proposal

Abstract

The ability to reliably distribute entanglement among the nodes of a network is an essential requirement for the development of effective quantum communication protocols and the realization of useful quantum networks. It has been demonstrated, in different contexts, that two remote systems can be entangled via local interactions with a carrier system that always remains in a separable state with respect to such distant particles. We develop a strategy for entanglement distribution via separable carriers that can be applied to any number of network nodes to achieve various entanglement distribution patterns. We show that our protocol results in multipartite entanglement, while the carrier mediating the process is always in a separable state with respect to the network. We provide examples showcasing the flexibility of our approach and propose a scheme of principle for the experimental demonstration of the protocol.

1. Introduction

The crucial role played by entanglement in quantum networking and communication has long been established through a plethora of groundbreaking protocols and experimental demonstrations [1–8]. It is therefore imperative that efficient methods of entanglement generation among the nodes of a quantum network are developed. In particular, we need protocols which take the fragility of entanglement into account, for instance, by creating this vital resource just before it is needed to be used.

Say we have two parties, Alice and Bob, who aim to share entanglement. To distribute entanglement directly, Alice would create an entangled state of two particles in her laboratory before sending one particle to Bob through a quantum channel. Alternatively, Alice and Bob could distribute entanglement indirectly through the use of an ancilla. This carrier system would first interact with Alice's particle in her laboratory, then be sent to Bob. This process will often require the carrier to become entangled with the two systems.

However, it is possible to entangle Alice and Bob's systems in this way without ever entangling either system with the ancilla. Theoretical proposals were put forward for entanglement distribution via separable states (EDSS) in the discrete-variable case [9, 10] and continuous-variable case [11–13] before it was demonstrated experimentally [14–16]. Recently, a continuous-variable approach also delivered a scheme for distribution of Gaussian entanglement and steering via separable states [17], followed by an experimental demonstration [18]. It is important to note that quantum discord is necessary for EDSS to be possible [19]. As discord is much more robust to noise and environmental effects than entanglement [20–24], EDSS provides an advantage over protocols which rely on the presence of entanglement. Interestingly, the fact that EDSS depends on non-classical correlations also means it can be used to detect non-classicality in inaccessible objects [25–27].

In what follows, we will build on Kay's EDSS protocol for qubits [10]. The procedure is as follows: Firstly, Alice and Bob initially share a separable state of their systems A and B. Secondly, Alice introduces an ancilla system K which is uncorrelated from AB. Thirdly, Alice performs the *encoding operation*, that is, a unitary

operation U_{AK} on her system and the carrier. Finally, Alice sends K to Bob. Kay [10] shows that when AB is initially in a Bell-diagonal state and U_{AK} is a controlled-phase gate, it is possible to choose a suitable initial state for K so that the state of the total system at the end of the protocol is entangled in the bipartition $A|BK$ and K remains separable from A and B throughout the process. In what follows, we add an extra step to the protocol; Bob performs a *decoding operation* on his particle and the carrier after he receives K from Alice. This results in entanglement in both the $A|BK$ and $B|AK$ bipartitions while the ancilla remains separable with no entanglement in the partition $K|AB$.

In this work, we generalize the protocol in [10] to the distribution of multipartite entanglement through EDSS, specifically focusing on the conditions of its experimental demonstration in [14]. Multipartite EDSS has previously been addressed in [28], where a systematic method was proposed based on the EDSS protocol by Cubitt *et al* [9]. In this case, AB and K are initially correlated (yet unentangled). The risk of entangling the bipartition $K|AB$ is therefore higher in their proposal and extra effort must be made to ensure its prevention. As the initial state of K in [10, 14] shares no classical or non-classical correlations with A or B, we avoid this problem and show that favoring this type of protocol offers a promising avenue for successful EDSS with fewer restrictions.

The remainder of this paper is structured as follows: In section 2, we introduce the protocol and show that the strategy relies on a particular initial state setting, that allows us to infuse the system with the initial quantum correlations necessary to obtain, at the end of the protocol, multipartite entanglement. In section 3 we show that this protocol can be applied to different entanglement distribution patterns and that, in general, it represents a very flexible approach to the problem of EDSS. In addition, in section 4, we propose two possible experimental platforms for the implementation of such a protocol in a photonic scenario. Finally in section 5 we present our conclusions.

2. Illustration of the protocol

2.1. Two-qubit protocol

We will refer explicitly to the version of the protocol for EDSS that has been reported in [14] as illustrated in figure 1. In such a scheme, the initial state of the two nodes A and B is separable, yet features non-classical correlations (as quantified by quantum discord [19]). Explicitly, we take,

$$\alpha_{AB} = \frac{1}{4}\left(|00\rangle\langle 00| + |11\rangle\langle 11|\right) + \frac{1}{8}\left(|DD\rangle\langle DD| + |AA\rangle\langle AA| + |RL\rangle\langle RL| + |LR\rangle\langle LR|\right)_{AB}, \tag{1}$$

where $|D\rangle = \frac{1}{\sqrt{2}}(|0\rangle + |1\rangle)$, $|A\rangle = \frac{1}{\sqrt{2}}(|0\rangle - |1\rangle)$, $|R\rangle = \frac{1}{\sqrt{2}}(|0\rangle + i|1\rangle)$ and $|L\rangle = \frac{1}{\sqrt{2}}(|0\rangle - i|1\rangle)$. While α_{AB} is invariant under partial transposition, it is endowed with non-zero quantum discord, as quantified by the relative entropy of discord [29, 30]:

$$\mathcal{D}(\alpha_{AB}) = \min_{\Pi_B}[S(\Pi_B(\alpha_{AB}))] - S(\alpha_{AB}), \tag{2}$$

where $S(\rho)$ is the von Neumann entropy of state ρ and $\Pi_B(\rho) = \sum_{j=0}^{1}\pi_j\rho\pi_j$ is a rank-one projective measurement of ρ with $\pi_{0,1}$ two orthogonal projectors on qubit B. We have $\mathcal{D}(\alpha_{AB}) = 0.0612781$.

The state of the nodes is then subjected to encoding and decoding operations, each consisting of a controlled-phase (CPHASE) gate acting on the joint state of one node Q (either A or B) and the carrier K as

$$\text{CPHASE} := |0\rangle\langle 0|_Q \otimes \mathbb{1}_K + |1\rangle\langle 1|_Q \otimes \sigma_{z,K} \tag{3}$$

where $\mathbb{1}$ is the two-dimensional identity matrix and σ_z the z Pauli matrix. This gate sets a relative phase between the two states of the computational basis of the target qubit K, depending on the state of control one Q.

The initial state of the latter must be a mixture of orthogonal vectors that are maximally distant from the eigenstates of the Pauli matrix σ_z, in order to amplify the effect of the encoding and decoding operations.

We thus choose,

$$\alpha_K = \frac{1}{4}\left(|D\rangle\langle D| + 3\,|A\rangle\langle A|\right)_K, \tag{4}$$

although a mixture of $|R\rangle$ and $|L\rangle$ would also be suitable. These mixing probabilities are chosen so as to guarantee that the carrier is not entangled throughout the process, while achieving the largest possible entanglement between the two nodes at the end of the protocol. In this sense, a mixture with balanced probabilities would be suitable too, although less effective.

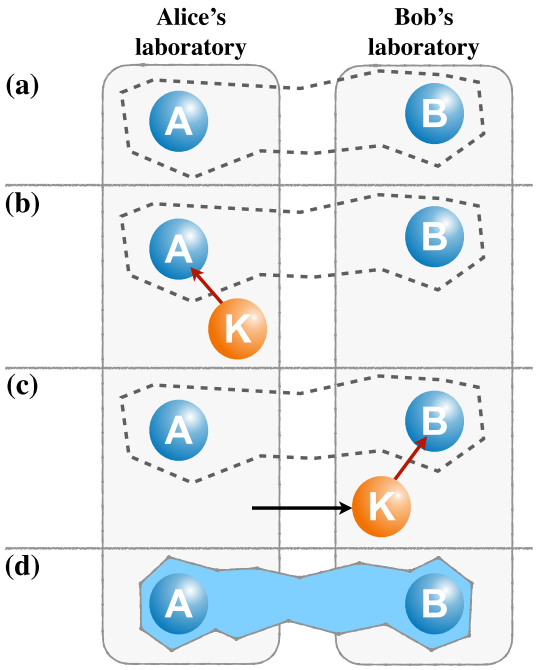

Figure 1. Diagram of the two-qubit protocol. (a) Nodes A and B are initially separable and they share quantum discord (dashed line). (b) Alice introduces the carrier K which is completely uncorrelated from AB. The encoding operation, in this case a controlled-phase gate, is performed between A and K. (c) Carrier K is sent to Bob and B and K interact via the decoding operation. (d) Particles A and B now share quantum entanglement.

The protocol now involves the encoding step, when the CPHASE gate is applied to qubit A and the carrier. This is then followed by a decoding step, consisting of the application of the CPHASE to node B and carrier. The first step reads:

$$\beta_{ABK} = \mathcal{P}_{AK}(\alpha_{AB} \otimes \alpha_K)\mathcal{P}_{AK}^{\dagger}, \tag{5}$$

where

$$\mathcal{P}_{AK} = |0\rangle\langle 0|_A \otimes \mathbb{1}_K + |1\rangle\langle 1|_A \otimes \sigma_{z,K}, \tag{6}$$

is the CPHASE gate between A and the carrier K. The decoding step then gives:

$$\gamma_{ABK} = \mathcal{P}_{BK}\beta_{ABK}\mathcal{P}_{BK}^{\dagger}. \tag{7}$$

The resulting state γ_{ABK} features distillable entanglement in the bipartitions $A|BK$ and $B|AK$ with the carrier K being in a separable state with respect to the state of the nodes (either collectively or individually taken).

2.2. General protocol

We now exploit the same encoding and decoding mechanisms illustrated above to design a generalization of the two-qubit protocol to a multipartite set of nodes. The resource being exploited is a mixed state that features initial non-classical correlations between each of the node pairs. The scope of the process is to entangle the elements of the network.

2.2.1. Initial state of the network, carrier state, and encoding-decoding operations

We consider the case of a network of N nodes $\{Q_i\}$ $(i = 1, \ldots, N)$ and investigate the arrangement of a protocol capable of establishing a pattern of entangled links between such nodes, according to a given structure. Thus, we require the definition of a state which features non-classical correlations between the nodes we wish to get entangled. In order to do that, we use the two-qubit state featuring quantum discord that was employed in the two-qubit case of equation (1).

Proceeding in analogy with the bipartite case, we generalize this state to N qubits by imposing a mixed initial state, consisting of a balanced mixture of terms featuring non-classicality between every pair of nodes targeted by our protocol. Each of such terms features a correlated state of a given pair of nodes, while the other nodes are set in an eigenstate of the encoding and decoding operation. We define a list of two-element sets containing the M pairs we wish to entangle, labeling them as $\{\mathcal{C}_k\}_{k=1}^{M}$, where each $\mathcal{C}_k = \{Q_i, Q_j\}$

represents a different node pair $\{i,j\}$ among the chosen ones. The initial state of the network α_N has thus the form:

$$\alpha_N = \frac{1}{M}\sum_{k=1}^{M} \rho^0_{\mathcal{C}_k} \left(\bigotimes_{Q_i \notin \mathcal{C}_k} \alpha^0_{Q_i} \right), \tag{8}$$

where $\alpha^0_{Q_i} = |0\rangle\langle 0|_{Q_i}$ and $\rho^0_{\mathcal{C}_k}$ is the initial state in equation (1), but for the pair $\mathcal{C}_k$. For instance, we can choose to distribute entanglement according to a chain-like structure, namely a linear network in which each node is entangled with its closest neighbors. The initial state can be written in the compact form as:

$$\alpha_N^{linear} = \frac{1}{N-1}\sum_{k=1}^{N-1} \rho^0_{Q_k,Q_{k+1}} \left(\bigotimes_{Q_i \neq \{Q_k,Q_{k+1}\}} \alpha^0_{Q_i} \right). \tag{9}$$

Such an initial state is necessary to keep the carrier in a separable state with respect to the network. Basically, in this way we are able to carry the two-qubit protocol in parallel over any node pair we want to entangle, without interference between the various terms. As we will see later on, this has some interesting implications for the features of the final state.

The encoding and decoding operations consist of CPHASE gates $\mathcal{P}_{Q_iK}$ acting on the state of node Q_i and the carrier K, whose initial state is chosen again as in equation (4). Other equivalent gate-carrier initial state pairings exist, though they do not result in better performance of the protocol.

2.2.2. Single qubit carrier

In this case, we only have one carrier K and the total initial state of the system can be set as:

$$\alpha_T = \alpha_N \otimes \alpha_K, \tag{10}$$

so that the preparation of the network system and the carrier can be independently addressed. As the carrier is the same for each pair of nodes, a single encoding and decoding step for each qubit is enough for weaving multiple entanglement links. The effect of the local CPHASE gate on the total state is:

$$\mathcal{P}_{Q_lK}\alpha_T\mathcal{P}^\dagger_{Q_lK} = \frac{1}{M}\sum_{k=1}^{M} \chi_{k,Q_l} \left(\bigotimes_{Q_i \notin \mathcal{C}_k} \alpha^0_{Q_i} \right), \tag{11}$$

where

$$\chi_{k,Q_l} = \begin{cases} \rho^0_{\mathcal{C}_k} \otimes \alpha_K & \text{for } Q_l \notin \mathcal{C}_k, \\ \mathcal{P}_{Q_lK}\left(\rho^0_{\mathcal{C}_k} \otimes \alpha_K\right)\mathcal{P}^\dagger_{Q_lK} & \text{for } Q_l \in \mathcal{C}_k. \end{cases} \tag{12}$$

The CPHASE gate on qubit Q_l acts as an encoding operation on the terms involving Q_l as a target or a decoding one, while acting as the identity on the others.

2.2.3. Multiple qubit carriers

It is possible to tailor the above protocol to work with multiple carriers. We also investigate this case in order to understand which beneficial effects and costs derive from this choice. We consider compound of n qubits $\{K_i\}_{i=1}^n$ and take as initial state for each the state α_K in equation (4). This sets the total product state of the carrier compound as:

$$\alpha_{\bar{K}} = \bigotimes_{i=1}^{n} \alpha^i_K = \bigotimes_{i=1}^{n} \left(\frac{1}{4}|D\rangle\langle D|_{K_i} + \frac{3}{4}|A\rangle\langle A|_{K_i} \right), \tag{13}$$

so that the total initial state is simply

$$\alpha_T = \alpha_N \otimes \alpha_{\bar{K}}. \tag{14}$$

The main difference with respect to the one qubit carrier protocol is that, in the present case, we proceed to entangle each qubit pair making them interact with a different carrier. Therefore, node qubit Q_i is subject to encoding via the carrier qubit K_i, which also mediates the local decoding at Q_{i+1}. Then, the encoding between Q_{i+1} and Q_{i+2} is mediated by carrier K_{i+1}. Therefore, different encoding and decoding operations are needed.

In general, the final state of the nodes will have the form of a mixture of terms stemming from the various two-qubit processes, which could take place in parallel, and an incoherent term Ω_N, thus reading:

$$\rho_N^f = P\Omega_N + (1-P)\sum_{k=1}^{M} \left|\phi^+\right\rangle\left\langle\phi^+\right|_{\mathcal{C}_k} \left(\bigotimes_{Q_i\notin\mathcal{C}_k} \alpha^0_{Q_i}\right), \tag{15}$$

where $|\phi^+\rangle = \frac{1}{\sqrt{2}}(|00\rangle + |11\rangle)$ is a Bell state and, as stated previously, $\{\mathcal{C}_k\}_{k=1}^M$ is the list of node pairs we aim to entangle. The mixing coefficient P is determined by the terms we insert in the initial mixed states, hence the number of entangled links we wish to establish. For each contribution, an incoherent residual term appears in the final state, forming the global incoherent term Ω_N. Therefore, the final state is a mixture of terms featuring bipartite entanglement, one for each of the initially non-classically correlated node pairs. Clearly, that implies a probabilistic generation of entanglement. Nevertheless, as we explicitly show in the following examples, the final state of the system unambiguously exhibit multipartite entanglement, namely the network is entangled with respect to any possible bipartition.

3. Analysis of performance

In this section, we analyze the performance of both single- and multiple-carrier protocols by addressing two explicit examples.

3.1. Four nodes example: ring configuration

3.1.1. Single carrier

We investigate a four-node case where the qubits $Q_{1,\dots,4}$ are entangled as a result of the application of the protocol illustrated before. As we request explicitly that Q_1 and Q_4 are entangled, we would thus realize a *ring-like* structure (cf figure 2(a)). The initial state of the nodes, then, must include non-classical correlations between every possible pair $\{\mathcal{C}_k\}_{k=1}^4$, where $\mathcal{C}_k = \{Q_k, Q_{k+1}\}$ and we set $Q_5 = Q_1$, so that:

$$\alpha_4 = \frac{1}{4}\left(\rho^0_{Q_1,Q_2}\otimes\alpha^0_{Q_3}\otimes\alpha^0_{Q_4} + \rho^0_{Q_2,Q_3}\otimes\alpha^0_{Q_1}\otimes\alpha^0_{Q_4} + \rho^0_{Q_3,Q_4}\otimes\alpha^0_{Q_1}\otimes\alpha^0_{Q_2} + \rho^0_{Q_4,Q_1}\otimes\alpha^0_{Q_2}\otimes\alpha^0_{Q_3}\right), \tag{16}$$

where $\rho^0_{\mathcal{C}_k}$ and $\alpha^0_{Q_i}$ are the same as in equation (8). The protocol consists of only four steps, taking the initial state α_4 to the final one as:

$$\eta_4 = \left(\Pi_{j=1}^4 \mathcal{P}_{Q_jK}\right)(\alpha_4\otimes\alpha_K)\left(\Pi_{j=1}^4 \mathcal{P}^\dagger_{Q_jK}\right). \tag{17}$$

In particular, the amount of entanglement in each of the one-vs-four bipartitions of the form $Q_j|\mathcal{G}_K$ with $\mathcal{G}_K = \{Q_1,Q_2,Q_3,Q_4,K\}\setminus Q_j$ that can be identified in state η_4 is the same: the corresponding partially transposed density matrices $\eta^{\mathrm{PT}_{Q_j}}$ all have a single negative eigenvalue equal to -0.0175206, so that the entanglement $\mathcal{E}_{Q_j|\mathcal{G}_K}$ does not depend on $j = 1,\dots,4$. On the other hand, the entanglement $\mathcal{E}_{K|Q_{1,\dots,4}}$ between the carrier K and the network is identically zero, thus achieving a successful distribution of entanglement without involving the carrier. It is worth noting that after projecting the carrier system onto state $|A\rangle$ and tracing the carrier system away we obtain a reduced matrix of the network only which exhibit the same entanglement values. In order to demonstrate that the system actually features multipartite entanglement, we check the eigenvalues of the partially transposed state with respect to any possible bipartition of the system. Such entanglement witness directly stems from the Peres-Horodecki separability criterion [31, 32], from which we know that a negative eigenvalue of the partially transposed density matrix of a bipartite system witnesses entanglement between the parties. As reported in table 2, we fulfill this requirement for all possible bipartitions.

3.1.2. Multi-qubit carrier

We now move to the study of a multi-carrier configuration, and how this might affect the effectiveness of the protocol. As in the ring pattern we have to weave four entanglement links. We thus consider a compound carrier system of 4 qubits K_j $(j = 1,\dots,4)$. The protocol differs from the single-carrier one in the exploitation of different carrier subspaces for the encoding and decoding operations affecting different node pairings. This implies that each operation will only act on a certain link, depending on the nodes that are involved. Therefore, the protocol needs twice the number of steps required in the single-qubit carrier scheme. Such steps are explicitly illustrated in table 1.

We report a sketch of the procedure in figure 2(b). We compute again the eigenvalues for any possible bipartition of the system, reporting them in table 2. The results of our analysis show that also a qudit carrier

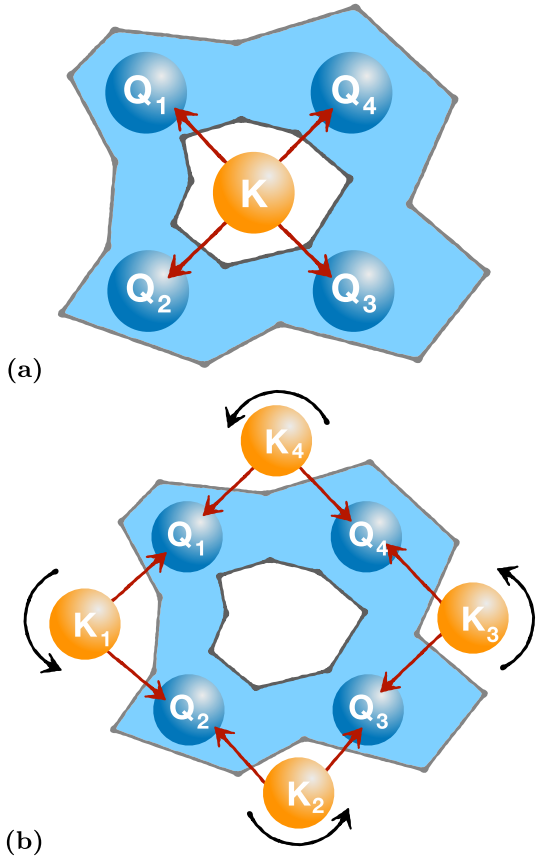

Figure 2. Ring topology protocols. (a) Single-carrier protocol: the carrier qubit K interacts once with each node; (b) qudit carrier case: the carrier travels in one direction, interacting twice with each node, once for encoding and the second time for decoding, since the encoding and decoding steps involve different subspaces of the carrier.

Table 1. Description of the steps required in a multi-qubit carrier protocol. We provide the label of the state achieved at each step of the scheme, the corresponding encoding (decoding) operation and the associated encoder (decoder).

State label	Description of evolution	Encoder/decoder
β_T	$\mathcal{P}_{Q_1\,K_1}\alpha_T\mathcal{P}^{+}_{Q_1\,K_1}$	K_1
γ_T	$\mathcal{P}_{Q_2\,K_1}\beta_T\mathcal{P}^{+}_{Q_2\,K_1}$	K_1
δ_T	$\mathcal{P}_{Q_2\,K_2}\gamma_T\mathcal{P}^{+}_{Q_2\,K_2}$	K_2
η_T	$\mathcal{P}_{Q_3\,K_2}\delta_T\mathcal{P}^{+}_{Q_3\,K_2}$	K_2
ζ_T	$\mathcal{P}_{Q_3\,K_3}\eta_T\mathcal{P}^{+}_{Q_3\,K_3}$	K_3
κ_T	$\mathcal{P}_{Q_4\,K_3}\zeta_T\mathcal{P}^{+}_{Q_4\,K_3}$	K_3
χ_T	$\mathcal{P}_{Q_4\,K_4}\kappa_T\mathcal{P}^{+}_{Q_4\,K_4}$	K_4
ω_T	$\mathcal{P}_{Q_1\,K_4}\chi_T\mathcal{P}^{+}_{Q_1\,K_4}$	K_4

approach produces multipartite entanglement. Indeed, as we show in table 2, the eigenvalues of the partially transposed density matrix, with respect to any bipartition of the nodes system, are negative. A main drawback comes from the fact that, although the carrier is in a separable state, tracing it away presents some complications. Since each of the different entanglement links is mediated by a different subspace, the projection of the qubit carrier on the state $|A\rangle$ will result in the preservation of that link in the reduced network state. Unfortunately, that cannot be done simultaneously for all the node pairs: by projecting every qubit carrier on their respective $|A\rangle$ state, we get a separable reduced state of the network. Therefore, the final state for the system remains multipartite entangled as far as the carrier state is not further manipulated. The carrier can be only traced away in case we wish to observe a specific entanglement link between two nodes.

3.1.3. General remarks on ring topology protocols

In order to compare the effectiveness of the two protocols we compute the average negativity of the final state for both cases. Given a certain partition p of a composite state ρ, we can define negativity as in [33]:

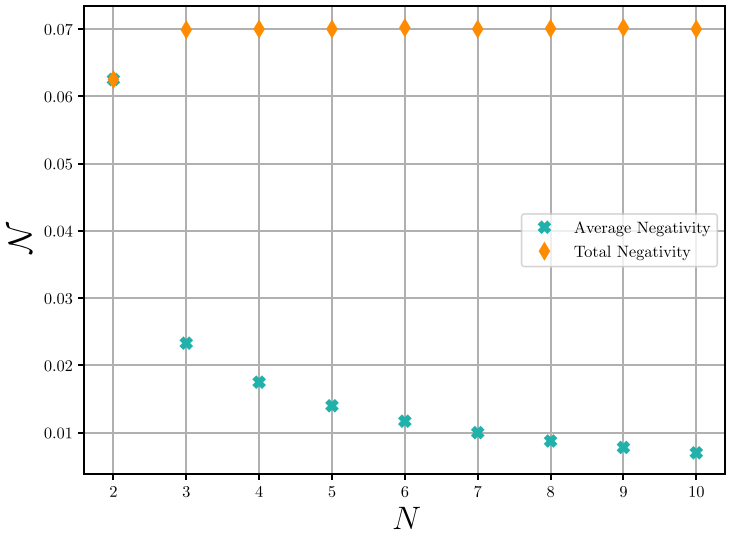

Figure 3. Negativity vs number of network nodes. The average negativity $\mathcal{N}$ is reported in function of the number of nodes N involved in the entanglement distribution protocol together with the corresponding total negativity Tot$\mathcal{N}$. The investigation is carried for the single qubit carrier case, in the ring pattern scenario.

$$\mathcal{N}_p(\rho) = \frac{||\rho^{T_p}|| - 1}{2}, \tag{18}$$

which is equal to the sum of all negative eigenvalues of the transposition of ρ with respect to the partition p. We consider the geometrical average of the negativity values for all the possible partitions of the system, denominating this value $\mathcal{N} = \sqrt{\prod_{\{p\}} \mathcal{N}_p(\rho)}$. We obtain a $\mathcal{N} = 0.0184179$ ($\mathcal{N} = 0.0261631$) for the single qubit carrier (multi-qubit carrier) protocol. These results show some advantage coming from the employment of a high-dimensional carrier in terms of entanglement production, though implying, in the perspective of an experimental realization, far heavier efforts and drawbacks.

It is worth noting that the amount of entanglement produced on average for a single link is lower than in the binary case of [14]. This is understandable considering the fact that the 4-nodes initial mixed state contains many more terms which generate 'noise' contributions in the final state, with respect to the 2 nodes case. Indeed, we expect the average produced negativity to decrease as the number of nodes increases, together with the number of terms to be included in the initial state. It may even be possible that, after a certain size of the network, entanglement between the nodes is no longer detectable. Nonetheless, the total negativity we produce, defined as the sum of all the negative eigenvalues over any bipartition Tot $\mathcal{N} = \sum_{\{p\}} \mathcal{N}_p$, should not change: indeed, the initial state always features the same amount of initial quantum correlation, which is the same as the two qubit case, even if split among a larger number of terms in the total mixture. We investigate the ring pattern case up to $N = 10$ nodes, in order to understand the trend of negativity in function of the size of the network, reporting the results in figure 3. Our simulations confirm the expected decrease of the average negativity, but also highlights that the total negativity remains constant as we increase the number of entangled nodes; therefore, the addition of more nodes does not seem to jeopardize the protocol efficiency in converting discord into entanglement.

3.2. Four nodes example: star topology

In order to provide a more thorough analysis of the potentialities of our approach, we tailor the protocol to generate a star-like entanglement pattern. We design the initial state and the protocol steps with the aim of producing a final state in which one central node is entangled with all the others. In this case, the final state results in entanglement with respect to any possible bipartition of the system. We briefly report on this analysis, because of the many analogies with the ring pattern case. We consider four nodes $\mathcal{Q} = \{Q_1, Q_2, Q_3, Q_4\}$, with Q_1 as the central node. Hence, our initial state has to be the mixture of three terms, each featuring non-classical correlation between qubit Q_1 and the others:

$$\alpha_4 = \frac{1}{3} \sum_{j=2}^{4} \rho^0_{Q_1,Q_j} \otimes \left(\bigotimes_{\bar{j} \in \overline{\mathcal{Q}}} \rho_{Q_{\bar{j}}} \right), \tag{19}$$

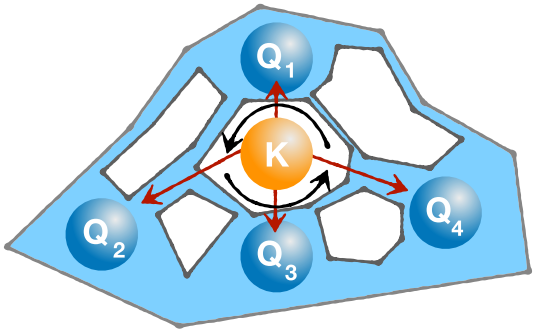

Figure 4. Star topology protocol. Single qubit carrier case: the qubit travels in one direction, interacting once with each node. We refer to the main body of the manuscript for a description of the qudit carrier case.

with $\overline{\mathcal{Q}} = \mathcal{Q}\backslash\{Q_1, Q_j\}$. In this case, the single qubit carrier protocol proceeds identically to the ring case: the carrier interacts at first with the central node and then once with each other qubit, as depicted in figure 4, since the first operation acts as encoding for every entanglement link. The only difference consists of the initial state preparation of the network, a remarkable feature in terms of flexibility of our strategy.

The qudit carrier case is more complex: each encoding and decoding operation have to be addressed separately, having the nodes interact with different sub-qubits of the carrier. Therefore, the carrier has to travel back and forth from the central node to the periferic qubits, until each link has been woven. Considering an eight-dimensional qudit carrier and three qubit subsystems K_1, K_2 and K_3, we can explicitly write down the protocol:

$$\begin{aligned}
&\beta_T = \mathcal{P}_{Q_1\,K_1}\alpha_T\mathcal{P}^{+}_{Q_1\,K_1}\ \text{encoding mediated by } K_1\\
\rightarrow\ &\gamma_T = \mathcal{P}_{Q_2\,K_1}\beta_T\mathcal{P}^{+}_{Q_2\,K_1}\ \text{decoding mediated by } K_1\\
\rightarrow\ &\delta_T = \mathcal{P}_{Q_1\,K_2}\gamma_T\mathcal{P}^{+}_{Q_1\,K_2}\ \text{encoding mediated by } K_2\\
\rightarrow\ &\eta_T = \mathcal{P}_{Q_3\,K_2}\delta_T\mathcal{P}^{+}_{Q_3\,K_2}\ \text{decoding mediated by } K_2\\
\rightarrow\ &\zeta_T = \mathcal{P}_{Q_1\,K_3}\eta_T\mathcal{P}^{+}_{Q_1\,K_3}\ \text{encoding mediated by } K_3\\
\rightarrow\ &\kappa_T = \mathcal{P}_{Q_4\,K_3}\zeta_T\mathcal{P}^{+}_{Q_4\,K_3}\ \text{decoding mediated by } K_3.
\end{aligned} \tag{20}$$

We report in table 3 the negative eigenvalues relative to every bipartition of the system for both methods. The average negativity computed from these results reads $\mathcal{N} = 0.019268$ for the qubit carrier protocol and $\mathcal{N} = 0.0262659$ for the qudit carrier one. In this case, the gap in entanglement production due to the exploitation of a high-dimensional carrier is slightly lower with respect to the ring pattern case, while the other issues remain. In general, the comparison between the usage of a qubit or a qudit carrier may provide different answers according to the application case and, more importantly, the actual experimental situation we are dealing with.

4. Experimental proposals

We propose some feasible experimental ways of demonstrating the effectiveness of our protocol in an optical framework.

4.1. Single qubit carrier

The direct experimental implementation of the single qubit carrier may well be a direct generalization of the apparatus of [14]: N single photons are employed, one as a carrier qubit, while the others act as the network nodes. The state of the network is encoded in the polarization degree of freedom of photons. All photons have to be indistinguishable with the carrier (hence reciprocally indistinguishable) in order to implement the optical quantum CZ gate as described in [14, 34], which acts as the encoding/decoding operation. That may be very difficult to obtain for a high number of photons: they have to be synchronized and identical in any degree of freedom. Indeed, it is possible to build sources with a such a control on the photon generation, which allow many photons interaction [35]. In figure 5, we report a sketch of the possible experimental implementation of the protocol for the ring pattern for three nodes. After each encoding/decoding operation the photon acting as carrier is sent to the next node and interacts with the corresponding photon, until it has interacted with all the network nodes and it can be projected and measured, leaving, in principle, an entangled state of the network. The most complex part of the protocol resides in the state preparation, but, if

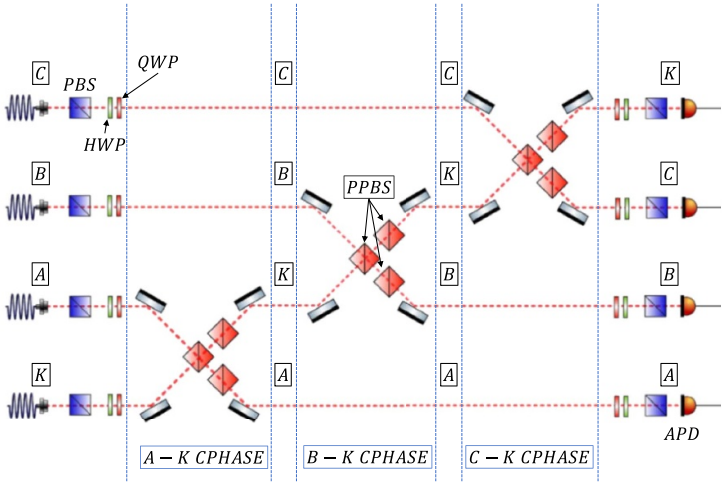

Figure 5. Scheme of principle for the distribution protocol for a 3 nodes ring pattern. Four indistinguishable photons must be harnessed, with a likely necessary further one for heralding. Three of them act as nodes and interact in turn with the fourth photon, acting as the carrier qubit. Initial state preparation in the degree of freedom of polarization can be addressed through the sequence of optical elements: Polarizing Beamsplitter, Half-wave Plate and Quarter-wave plate. The interaction between qubits can be implemented via the optical CPHASE gate described in [14, 34]. The sequence of physical interactions between the photons shall yield as a result a ring-like multipartite entanglement structure, or even a star-like structure, according to the initial state being implemented.

we wish to provide a mere experimental demonstration of the protocol effectiveness, the mixing probabilities of the various terms in the initial state may be simulated by different sampling times, as already done in [14]. That could not be the case in actual application scenarios.

4.2. Single qubit carrier, relay scheme

The request of producing N indistinguishable photons, even for low $N > 3$, may actually be difficult to comply with. There is another suitable way to demonstrate the protocol in an experimental implementation: in appendix B we report on a variation of the protocol, relying on a 'relay scheme', where the single qubit carrier is measured and replaced after a certain number of protocol steps. This scheme is less efficient than the standard one, but possesses some interesting features as we face an experimental realization. Indeed, the relay strategy implies that the carrier needs only to be indistinguishable with the qubit nodes it interacts with. In particular, we consider the case in which a new qubit carrier is employed after the previous one has interacted with two nodes. Therefore, again in an optical framework, we only need to generate three indistinguishable photons, plus a triggering one, which corresponds to what has been already realized in [14] for the binary protocol. The N nodes protocol may be realized by exploiting $N/2$ sources in an actual scenario.

In case of a proof-of-principle framework, it would be even possible to use the same photon source, since the different parts of the systems remain completely isolated throughout the protocol. It would only be necessary to suitably set the photons' state as the qubit pair which is simulated to be under observation. A sketch of the possible experimental implementation of the scheme for the case of the ring pattern in four nodes is reported in figure 6.

5. Concluding remarks

We have presented a scheme for the achievement of EDSS in a multipartite network. In contrast with the proposal in [28], where the carrier is made separable by additional operations, our strategy is a generalization of the one proposed in [14]: the carrier is always separable throughout the protocol and there is no need for supplemental manipulation of the carrier system, aimed at disentangling it. It is also characterized by a remarkable flexibility in terms of feasible distribution patterns and possible variations of the standard scheme. Indeed, our strategy may be extended to a continuous-variable framework, as in the binary case, in order to make experimental implementations easier to realize. The results of our work provide a very general alternative approach to direct protocols in the problem of entanglement distribution, although, as highlighted in the text, it is a probabilistic approach. Nevertheless, the advantages of using a separable state carrier in some environmental conditions [14], may be finally extended to the N qubits scenario, where noise can play a very relevant part. Therefore, these results may pave the way to the development of the general and useful application of EDSS protocols in actual multiparty Quantum Communication and Information tasks.

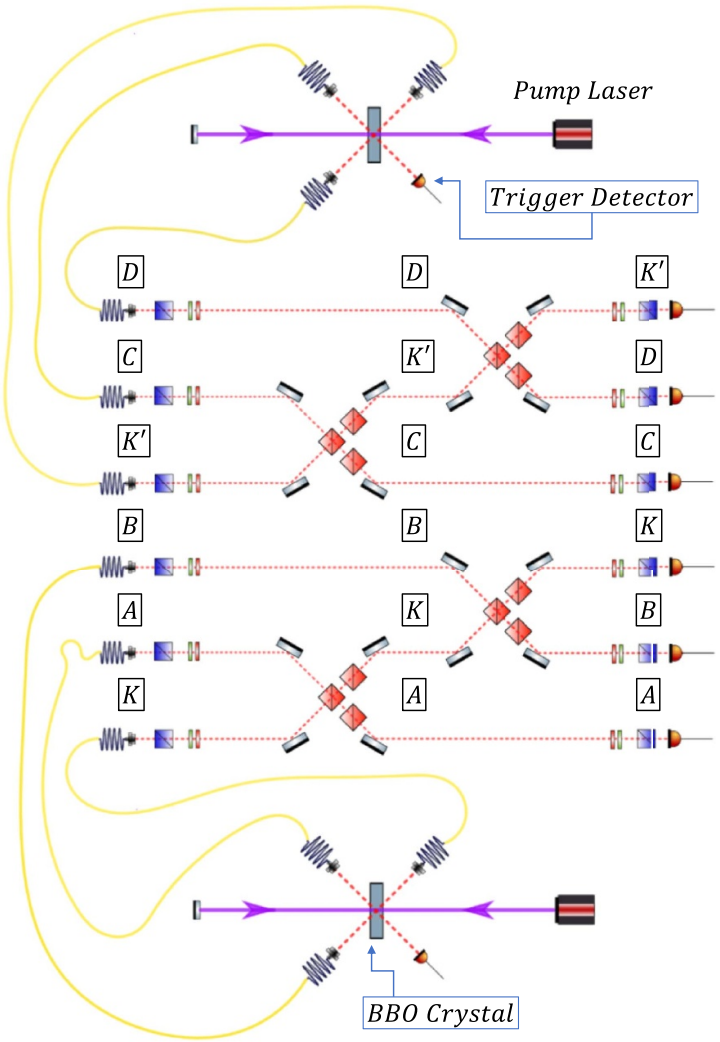

Figure 6. Scheme of principle for the Relay Protocol for a 4 nodes ring pattern. Two BBO crystals pumped by a pulsed laser generate four indistinguishable photons altogether. Three of them are sent into the setup, while the fourth is used to witness as a herald for generation. Two sources allow to generate two triplets of indistinguishable photons, each of which can be used to address two nodes and one carrier. The photons are prepared in the suitable initial state after traveling through an optical fiber, then three of them are used to perform the encoding and decoding of entanglement between A and B via K. After the measurement of K, a second triplet can be used to weave the entanglement between C and D via K' and, concurrently, the links between B and C and D and A.

For instance, an application of this work worth highlighting is quantum conference key agreement (QCKA) [36], that is, the ability to use properties of quantum states to securely share secret keys between $N > 2$ parties. Quantum key distribution is becoming increasingly important as we approach the realization of quantum computers which would render existing security protocols useless. In particular, QCKA is growing in relevance as quantum networks of many nodes are being developed for the purpose of secure communication (for instance, see [37–39]).

Remarkably, the resources for QCKA are precisely states with the entanglement structure achieved through the protocol illustrated here [40]. Once the entangled state has been shared among the desired N nodes according to the protocol in section 2, the N-BB84 protocol [36, 41] for QCKA could then be used to establish a secret key. Therefore, not only can we distribute keys securely between N parties without needing to send, for instance, fragile GHZ states to several nodes, but we show that it is in fact possible without sending any entanglement at all.

Data availability statement

The data that support the findings of this study are openly available at the following URL/DOI: https://doi.org/10.17034/00d54cd4-e164-4376-9757-ae2ed9010862.

Acknowledgments

We wish to thank professor Paolo Mataloni for facilitating and supporting the visit of A.L. to the School of Mathematics and Physics during which this work has started. We acknowledge support from the European Union's Horizon 2020 FET-Open project TEQ (766900), the Horizon Europe EIC-Pathfinder project QuCoM (101046973) and Innovate UK for the Horizon Europe guarantee—EIC 2021 (10032229), the Leverhulme Trust Research Project Grant UltraQuTe (Grant RGP-2018-266), the Royal Society Wolfson Fellowship (RSWF/R3/183013), the UK EPSRC (Grant No. EP/T028424/1) and the Department for the Economy Northern Ireland under the US-Ireland R&D Partnership Programme.

Appendix A. Simultaneously entangled pairs

At the end of section 3, we described the form of the final state of the network as a mixture of terms featuring entanglement between a single node pair each. Clearly, the initial state can be tailored to obtain different mixtures. We show this via a ring pattern example, where we consider a network of N nodes $\{Q_i\}_{i=1}^{N}$, where we consider N to be even for sake of simplicity. We want to obtain a final state of the network featuring multipartite entanglement and the possibility of having simultaneously entangled node pairs in the system. We set the initial state as the mixture of two terms:

$$\alpha_N = \frac{1}{2}\left(\bigotimes_{k=1}^{N/2}\rho_{Q_{2k-1},Q_{2k}} + \bigotimes_{j=0}^{N/2-1}\rho_{Q_{2j},Q_{2j+1}}\right), \tag{21}$$

where we consider $Q_0 = Q_N$. In this case, simply applying the single qubit carrier protocol, we would obtain a final state of the network fulfilling our initial requirements, but the carrier would end up being entangled during the process. Therefore, we mix these two terms with the initial state for a N nodes ring-like entanglement distribution pattern:

$$\begin{aligned}\alpha_N = \frac{1}{N+2}\Bigg[&\bigotimes_{k=1}^{N/2}\rho_{Q_{2k-1},Q_{2k}} + \bigotimes_{j=0}^{N/2-1}\rho_{Q_{2j},Q_{2j+1}} + \\ &+\sum_{k=1}^{N}\left(\bigotimes_{i=1}^{k}|0\rangle\langle 0|_{Q_i}\right)\otimes\rho^0_{Q_k,Q_{k+1}}\otimes\left(\bigotimes_{j=k+2}^{N}|0\rangle\langle 0|_{Q_j}\right)\Bigg],\end{aligned} \tag{22}$$

where we consider $Q_{N+1} = Q_1$. In this way, we are inserting 'noise' in the state of the system, which helps keep the carrier separable, while diminishing the probability of finding the network in a final state featuring simultaneously entangled node pairs. After the application of the single-qubit carrier protocol, the final state will be:

$$\begin{aligned}\rho^f_N = p\Omega_N + q&\left(\sum_{k=1}^{N}|\phi^+\rangle\langle\phi^+|_{Q_i,Q_{i+1}}\right)\otimes\left(\bigotimes_{j=1,j\neq i,i+1}^{N-1}\alpha^0_{Q_j}\right) \\ &+ r\left(\bigotimes_{k=1}^{N/2}|\phi^+\rangle\langle\phi^+|_{Q_{2k-1},Q_{2k}} + \bigotimes_{j=0}^{N/2-1}|\phi^+\rangle\langle\phi^+|_{Q_{2j},Q_{2j+1}}\right),\end{aligned} \tag{23}$$

where $p, q, r \in \mathcal{R}$ with $p+q+r=1$, and Ω_N is again a completely diagonal contribution to the state of the network, hence classical. Therefore, we have a certain probability of actually finding the system in the state we desire. Alternatively, if we relax the request of multipartite entanglement, we can use the initial state $\alpha = \bigotimes_{k=1}^{N/2}\rho_{Q_{2k-1},Q_{2k}}$, relatively increasing the probability of finding the network in a product state of entangled node pairs, although the system shall remain separable with respect to some bipartitions.

Appendix B. Relay scheme for single qubit carrier

It is possible to define a single qubit carrier scheme in which the carrier is halfway replaced with another qubit. This alternative protocol may result very useful for possible future experimental implementations, as highlighted in section 4. We explicitly show the details of this relay scheme in a four nodes ring pattern example. We have four nodes A, B, C, D and a carrier qubit K. The initial state of the network and carrier is

the same as in the standard ring pattern case α_T, as well as the encoding and decoding operations. The only difference consists of the fact that after two interactions, we project the qubit system on the $|A\rangle\langle A|$ state, we trace it away and we insert a new qubit carrier in the initial state α_K:

$$\begin{aligned}
&\beta_T = \mathcal{P}_{AK}\alpha_T\mathcal{P}_{AK}^{+}\\
\rightarrow\ &\gamma_T = \mathcal{P}_{BK}\beta_T\mathcal{P}_{BK}^{+}\\
\rightarrow\ &\gamma_T' = |A\rangle_K\langle A|\gamma_T|A\rangle_K\langle A|\\
\rightarrow\ &\gamma_N = Tr_K(\gamma_T')\\
\rightarrow\ &\gamma_T'' = \gamma_N\otimes\alpha_K'\\
\rightarrow\ &\delta_T = \mathcal{P}_{CK'}\gamma_T''\mathcal{P}_{CK'}^{+}\\
\rightarrow\ &\eta_T = \mathcal{P}_{DK'}\delta_T\mathcal{P}_{DK'}^{+}
\end{aligned} \tag{24}$$

At the end of the protocols, we get the following negative eigenvalues from the partial transpositions of η_T:

$$\begin{cases}
\mathcal{E}_{A-BCDK'} = \{-0.00986842, -0.00328947\}\\
\mathcal{E}_{B-ACDK'} = -0.00986842\\
\mathcal{E}_{C-ABDK'} = \{-0.00986842, -0.00328947\}\\
\mathcal{E}_{D-ABCK'} = -0.00986842\\
\mathcal{E}_{K'-ABCD} = 0
\end{cases} \tag{25}$$

and by analyzing all the partition the system exhibits multipartite entanglement. It is quite evident that the average negativity produced is lower than in the standard case, although the requested multipartite entanglement and carrier separability are achieved. Therefore, the relay scheme provides with a weaker yet effective protocol for EDSS, which may prove to be useful in practical applications.

Appendix C. Tables of eigenvalues

Table 2. Negative eigenvalues of every possible partition, ring pattern, qubit and qudit carrier protocols.

Bipartition	Single-carrier	Multiple-carrier
$Q_1\|Q_2Q_3Q_4K$	−0.0175 206	{−0.011786, −0.00392868, −0.00392868, −0.001309565}
$Q_2\|Q_1Q_3Q_4K$	−0.0175 206	{−0.011786, −0.00392868, −0.00392868, −0.001309565}
$Q_3\|Q_1Q_2Q_4K$	−0.0175 206	{−0.011786, −0.00392868, −0.00392868, −0.001309565}
$Q_4\|Q_1Q_2Q_3K$	−0.0175 206	{−0.011786, −0.00392868, −0.00392868, −0.001309565}
$Q_1Q_2\|Q_3Q_4K$	{−0.0078125, −0.0078125}	{−0.00769043, −0.00769043, −0.00286949, −0.00256348, −0.00256348, −0.00256348, −0.00256348, −0.000956497, −0.000956497, −0.000854492, −0.000854492, −0.000318832}
$Q_1Q_3\|Q_2Q_4K$	−0.03125	{−0.0117871, −0.0117871, −0.00395737, −0.00395737, −0.00395737, −0.00395737, −0.00195313}
$Q_1Q_4\|Q_2Q_3K$	{−0.0078125, −0.0078125}	{−0.00769043, −0.00769043, −0.00286949, −0.00256348, −0.00256348, −0.00256348, −0.00256348, −0.000956497, 0.000956497, −0.000854492, −0.000854492, −0.000318832}

Table 3. Negative eigenvalues of every possible partition, star pattern, qubit and qudit carrier protocols.

Bipartition	Single-carrier	Multiple-carrier
$Q_1\|Q_2Q_3Q_4K$	−0.0342865	{−0.0291511, −0.00642872, −0.00642872, −0.00642872}
$Q_2\|Q_1Q_3Q_4K$	−0.0121071	{−0.00681022, −0.00227007, −0.00227007, −0.000756691}
$Q_3\|Q_1Q_2Q_4K$	−0.0121071	{−0.00681022, −0.00227007, −0.00227007, −0.000756691}
$Q_4\|Q_1Q_2Q_3K$	−0.0121071	{−0.00681022, −0.00227007, −0.00227007, −0.000756691}
$Q_1Q_2\|Q_3Q_4K$	−0.0245719	{−0.0235657, −0.00681022, −0.00460722, −0.00460722, −0.00460722, −0.00227007}
$Q_1Q_3\|Q_2Q_4K$	−0.0245719	{−0.0235657, −0.00681022, −0.00460722, −0.00460722, −0.00227007}
$Q_1Q_4\|Q_2Q_3K$	−0.0245719	{−0.0235657, −0.00681022, −0.00460722, −0.00460722, −0.00460722, −0.00227007}

Appendix D. Separability of the carrier qubit

It can be shown that the state of the total system can be written as a separable decomposition with respect to the carrier qubit K at every stage of the protocol.

We begin with the two-qubit protocol in section 2, acting on the initial state $\alpha_{AB} \otimes \alpha_K$ with the encoding operation produces state β_{ABK}, which can be written as [14]

$$\begin{aligned}\beta_{ABK} = &\frac{3}{16}|00\rangle\langle 00| \otimes |A\rangle\langle A| + \frac{3}{16}|11\rangle\langle 11| \otimes |D\rangle\langle D| \\ &+ \frac{1}{8}|\phi^+\rangle\langle\phi^+| \otimes |0\rangle\langle 0| + \frac{1}{8}|\phi^-\rangle\langle\phi^-| \otimes |1\rangle\langle 1| \\ &+ \frac{1}{16}|01\rangle\langle 01| \otimes |A\rangle\langle A| + \frac{1}{16}|10\rangle\langle 10| \otimes |D\rangle\langle D| \\ &+ \frac{1}{16}|\phi^{+i}\rangle\langle\phi^{+i}| \otimes |L\rangle\langle L| + \frac{1}{16}|\phi^{-i}\rangle\langle\phi^{-i}| \otimes |R\rangle\langle R| \\ &+ \frac{1}{32}|01\rangle\langle 01| \otimes |L\rangle\langle L| + \frac{1}{32}|10\rangle\langle 10| \otimes |L\rangle\langle L| \\ &+ \frac{1}{32}|\psi^+\rangle\langle\psi^+| \otimes |R\rangle\langle R| + \frac{1}{32}|\psi^-\rangle\langle\psi^-| \otimes |R\rangle\langle R|,\end{aligned} \tag{26}$$

where $\{|\phi^{\pm}\rangle, |\psi^{\pm}\rangle\}$ is the Bell basis and $|\phi^{\pm i}\rangle = \frac{1}{\sqrt{2}}(|00\rangle \pm i|11\rangle)$. Therefore, the state β_{ABK} is separable with respect to the carrier at this point.

After performing the decoding operation, we achieve the state γ_{ABK} where

$$\begin{aligned}\gamma_{ABK} = &\frac{1}{4}|\phi^+\rangle\langle\phi^+| \otimes \frac{\mathbb{1}}{2} + \frac{3}{16}|00\rangle\langle 00| \otimes |A\rangle\langle A| \\ &+ \frac{3}{16}|11\rangle\langle 11| \otimes |A\rangle\langle A| + \frac{1}{16}|01\rangle\langle 01| \otimes |D\rangle\langle D| \\ &+ \frac{1}{16}|10\rangle|10\rangle \otimes |D\rangle\langle D| + \frac{1}{16}|\phi^+\rangle\langle\phi^+| \otimes |A\rangle\langle A| \\ &+ \frac{1}{16}|\phi^-\rangle\langle\phi^-| \otimes |D\rangle\langle D| + \frac{1}{16}|01\rangle\langle 01| \otimes \frac{\mathbb{1}}{2} \\ &+ \frac{1}{16}|10\rangle\langle 10| \otimes \frac{\mathbb{1}}{2},\end{aligned} \tag{27}$$

which demonstrates that this state too is separable with respect to K.

Moving to the four-qubit case in section 3, the ring structure has initial state in equation (16). Each element of the sum takes the form:

$$\frac{1}{4}\rho_{Q_iQ_j} \otimes |0\rangle\langle 0|_{Q_l} \otimes |0\rangle\langle 0|_{Q_m} \otimes \alpha_K. \tag{28}$$

A CPHASE gate with Q_l or Q_m as the control qubit will have no effect on this term. However, with Q_i as the control qubit, $\beta_{Q_iQ_jK} \otimes |0\rangle\langle 0|_{Q_l} \otimes |0\rangle\langle 0|_{Q_m}$ is generated. Alternatively, acting on Q_jK will give $\beta'_{Q_iQ_jK} \otimes |0\rangle\langle 0|_{Q_l} \otimes |0\rangle\langle 0|_{Q_m}$ where,

$$\begin{aligned}\beta' = &\beta - \frac{1}{16}|01\rangle\langle 01| \otimes |A\rangle\langle A| - \frac{1}{16}|10\rangle\langle 10| \otimes |D\rangle\langle D| \\ &+ \frac{1}{16}|01\rangle\langle 01| \otimes |D\rangle\langle D| + \frac{1}{16}|10\rangle\langle 10| \otimes |A\rangle\langle A|,\end{aligned} \tag{29}$$

and therefore is still a separable decomposition with respect to the carrier. When the CPHASE gate on Q_iK acts on the state $\beta'_{Q_iQ_jK}$, we retrieve $\gamma_{Q_iQ_jK}$.

Consequently, after the four CPHASE gates have been applied, the final state of the total system is:

$$\begin{aligned}\rho_{\text{final}} = &\gamma_{Q_1Q_2\ K} \otimes |0\rangle\langle 0|_{Q_3} \otimes |0\rangle\langle 0|_{Q_4} \\ &+ \gamma_{Q_2Q_3\ K} \otimes |0\rangle\langle 0|_{Q_4} \otimes |0\rangle\langle 0|_{Q_1} \\ &+ \gamma_{Q_3Q_4\ K} \otimes |0\rangle\langle 0|_{Q_1} \otimes |0\rangle\langle 0|_{Q_2} \\ &+ \gamma_{Q_4Q_1\ K} \otimes |0\rangle\langle 0|_{Q_2} \otimes |0\rangle\langle 0|_{Q_3}\,.\end{aligned} \tag{30}$$

For the star structure we have a similar effect; starting from the initial state in equation (19), we achieve the final state:

$$\rho_{\text{final}} = \frac{1}{3}\sum_{j=2}^{4} \gamma_{Q_1Q_jK} \left(\bigotimes_{\bar{j}\in\bar{\mathcal{Q}}} |0\rangle\langle 0|_{Q_{\bar{j}}} \right), \tag{31}$$

where $\bar{\mathcal{Q}} = \mathcal{Q}\backslash\{Q_1, Q_j\}$. Therefore, the carrier is separable from all other systems at each step of the protocol.

Extension to multi-qubit cases can be carried out following similar lines, but the proof is more involved and we omit it for the sake of simplicity.

ORCID iDs

Alessandro Laneve https://orcid.org/0000-0002-0416-5131
Mauro Paternostro https://orcid.org/0000-0001-8870-9134

References

[1] Ekert A K 1992 Quantum cryptography and Bell's theorem *Quantum Measurements in Optics* (Berlin: Springer) pp 413–8
[2] Bennett C H, Brassard G, Crépeau C, Jozsa R, Peres A and Wootters W K 1993 Teleporting an unknown quantum state via dual classical and Einstein-Podolsky-Rosen channels *Phys. Rev. Lett.* **70** 1895
[3] Cirac J I, Zoller P, Kimble H J and Mabuchi H 1997 Quantum state transfer and entanglement distribution among distant nodes in a quantum network *Phys. Rev. Lett.* **78** 3221
[4] Boschi D, Branca S, De Martini F, Hardy L and Popescu S 1998 Experimental realization of teleporting an unknown pure quantum state via dual classical and Einstein-Podolsky-Rosen channels *Phys. Rev. Lett.* **80** 1121
[5] Bouwmeester D, Pan J-W, Mattle K, Eibl M, Weinfurter H and Zeilinger A 1997 Experimental quantum teleportation *Nature* **390** 575
[6] Ursin R *et al* 2007 Entanglement-based quantum communication over 144 km *Nat. Phys.* **3** 481
[7] Humphreys P C, Kalb N, Morits J P, Schouten R N, Vermeulen R F, Twitchen D J, Markham M and Hanson R 2018 Deterministic delivery of remote entanglement on a quantum network *Nature* **558** 268
[8] Wengerowsky S, Joshi S K, Steinlechner F, Hübel H and Ursin R 2018 An entanglement-based wavelength-multiplexed quantum communication network *Nature* **564** 225
[9] Cubitt T S, Verstraete F, Dür W and Cirac J I 2003 Separable states can be used to distribute entanglement *Phys. Rev. Lett.* **91** 037902
[10] Kay A 2012 Using separableBell-diagonal states to distribute entanglement *Phys. Rev. Lett.* **109** 080503
[11] Mišta L Jr and Korolkova N 2008 Distribution of continuous-variable entanglement by separable Gaussian states *Phys. Rev.* A **77** 050302(R)
[12] Mišta L Jr and Korolkova N 2009 Improving continuous-variable entanglement distribution by separable states *Phys. Rev.* A **80** 032310
[13] Mišta L Jr 2013 Entanglement sharing with separable states *Phys. Rev.* A **87** 062326
[14] Fedrizzi A, Zuppardo M, Gillett G, Broome M, Almeida M, Paternostro M, White A and Paterek T 2013 Experimental distribution of entanglement with separable carriers *Phys. Rev. Lett.* **111** 230504
[15] Vollmer C E, Schulze D, Eberle T, Händchen V, Fiurášek J and Schnabel R 2013 Experimental entanglement distribution by separable states *Phys. Rev. Lett.* **111** 230505
[16] Peuntinger C, Chille V, Mišta L Jr, Korolkova N, Förtsch M, Korger J, Marquardt C and Leuchs G 2013 Distributing entanglement with separable states *Phys. Rev. Lett.* **111** 230506
[17] Xiang Y, Su X, Mišta L Jr, Adesso G and He Q 2019 Multipartite einstein-podolsky-rosen steering sharing with separable states *Phys. Rev.* A **99** 010104
[18] Wang M, Xiang Y, Kang H, Han D, Liu Y, He Q, Gong Q, Su X and Peng K 2020 Deterministic distribution of multipartite entanglement and steering in a quantum network by separable states *Phys. Rev. Lett.* **125** 260506
[19] Chuan T, Maillard J, Modi K, Paterek T, Paternostro M and Piani M 2012 Quantum discord bounds the amount of distributed entanglement *Phys. Rev. Lett.* **109** 070501
[20] Werlang T, Souza S, Fanchini F F and Boas C J V 2009 Robustness of quantum discord to sudden death *Phys. Rev.* A **80** 024103
[21] Ferraro A, Aolita L, Cavalcanti D, Cucchietti F M and Acín A 2010 Almost all quantum states have nonclassical correlations *Phys. Rev.* A **81** 052318
[22] Wang B, Xu Z Y, Chen Z Q and Feng M 2010 Non-Markovian effect on the quantum discord *Phys. Rev.* A **81** 014101
[23] Fanchini F F, Werlang T, Brasil C A, Arruda L G E and Caldeira A O 2010 Non-Markovian dynamics of quantum discord *Phys. Rev.* A **81** 052107

[24] Mazzola L, Piilo J and Maniscalco S 2010 Sudden transition between classical and quantum decoherence *Phys. Rev. Lett.* **104** 200401
[25] Krisnanda T, Zuppardo M, Paternostro M and Paterek T 2017 Revealing nonclassicality of inaccessible objects *Phys. Rev. Lett.* **119** 120402
[26] Krisnanda T, Marletto C, Vedral V, Paternostro M and Paterek T 2018 Probing quantum features of photosynthetic organisms *npj Quantum Inf.* **4** 60
[27] Krisnanda T, Tham G Y, Paternostro M and Paterek T 2020 Observable quantum entanglement due to gravity *npj Quantum Inf.* **6** 12
[28] Karimipour V, Memarzadeh L and Bordbar N T 2015 Systematics of entanglement distribution by separable states *Phys. Rev.* A **92** 032325
[29] Modi K, Paterek T, Son W, Vedral V and Williamson M 2010 Unified view of quantum and classical correlations *Phys. Rev. Lett.* **104** 080501
[30] Horodecki M, Horodecki P, Horodecki R, Oppenheim J, Sen(De) A, Sen U and Synak-Radtke B 2005 Local versus nonlocal information in quantum-information theory: formalism and phenomena *Phys. Rev.* A **71** 062307
[31] Peres A 1996 Separability criterion for density matrices *Phys. Rev. Lett.* **77** 1413
[32] Horodecki M, Horodecki P and Horodecki R 1996 Separability of mixed states: necessary and sufficient conditions *Phys. Lett.* A **223** 1
[33] Vidal G and Werner R F 2002 Computable measure of entanglement *Phys. Rev.* A **65** 032314
[34] Langford N K, Weinhold T J, Prevedel R, Resch K J, Gilchrist A, O'Brien J L, Pryde G J and White A G 2005 Demonstration of a simple entangling optical gate and its use inBell-state analysis *Phys. Rev. Lett.* **95** 210504
[35] Jones A E, Menssen A J, Chrzanowski H M, Wolterink T A W, Shchesnovich V S and Walmsley I A 2020 Multiparticle interference of pairwise distinguishable photons *Phys. Rev. Lett.* **125** 123603
[36] Murta G, Grasselli F, Kampermann H and Bruß D 2020 Quantum conference key agreement: a review *Adv. Quantum Technol.* **3** 2000025
[37] Liao S-K *et al* 2018 Satellite-relayed intercontinental quantum network *Phys. Rev. Lett.* **120** 030501
[38] Dynes J F *et al* 2019 Cambridge quantum network *npj Quantum Inf.* **5** 101
[39] Aguago A, López V, López D, Peev M, Poppe A, Pastor A, Folgueira J and Martín V 2019 The engineering of software-defined quantum key distribution networks *IEEE Commun. Mag.* **57** 20
[40] Carrara G, Kampermann H, Bruß D and Murta G 2021 Genuine multipartite entanglement is not a precondition for secure conference key agreement *Phys. Rev. Res.* **3** 013264
[41] Grasselli F, Kampermann H and Bruß D 2018 Finite-key effects in multipartite quantum key distribution protocols *New J. Phys.* **20** 113014